Available online at www.sciencedirect.com
ScienceDirect
Journal of Chromatography A, 1189 (2008) 355–365
JOURNAL OF CHROMATOGRAPHY A
www.elsevier.com/locate/chroma

Photodegradation of methyl green using visible irradiation in ZnO suspensions
Determination of the reaction pathway and identification of intermediates by a high-performance liquid chromatography–photodiode array-electrospray ionization-mass spectrometry method

F.D. Mai [b], C.C. Chen [a,*], J.L. Chen [b], S.C. Liu [b]

[a] *Department of General Education, National Taichung Nursing College, No. 193 Sec. 1, San-Min Road, Taichung 403, Taiwan, ROC*
[b] *Department of Biochemistry, School of Medicine, Taipei Medical University, Taipei 110, Taiwan, ROC*

Available online 17 January 2008

Abstract

Heterogeneous photocatalytic treatment of a dye called methyl green (MG), which was simulating textile wastewater from associated auxiliary chemicals, was investigated using ZnO. A detailed investigation of the photodegradation of MG has been carried out in the ZnO suspension irradiated with visible light. The effects of various factors – viz. pH values, amount of catalyst, initial dye concentration, and the presence of NaCl, Na_2CO_3, H_2O_2, and $Na_2S_2O_8$ – on the degradation efficiency were studied. Thirty-two intermediates were separated, identified, and characterized by high-performance liquid chromatography–photodiode array-electrospray ionization-mass spectrometry (HPLC–ESI-DAD-MS) technology, giving us insight into the pathways of the degradation process.

Keywords: ZnO; Photodegradation; Methyl green; HPLC–ESI-DAD-MS

1. Introduction

From an ecological and physiological point of view, the elimination of toxic chemicals from wastewater is currently one of the most important subjects in pollution control. Triphenylmethane dyes are used extensively in the textile industry for dyeing nylon, wool, cotton, and silk, as well as for coloring of oil, fats, waxes, varnish, and plastics. The paper, leather, cosmetic, and food industries consume a high quantity of triphenylmethane dyes of various kinds [1]. Cationic triphenylmethane dyes have found widespread use as colorants in industry and as antimicrobial agents [2]. Recent reports indicate that they may further serve as targetable sensitizers in the photo-destruction of specific cellular components or cells [3]. MG is a basic triphenylmethane-type dicationic dye, usually used for staining solutions in medicine and biology [4] and as a photochromophore to sensitize gelatinous films [5]. It has been used to differentiate between deoxyribonucleic acid and ribonucleic acid [6]. The binding of MG to DNA is probably ionic, as opposed to intercalative, and it remains so stably bound to double-stranded DNA that, with its conversion to the colorless carbinol from, it has been used to assess the binding of other molecules to DNA [7]. However, great concern has arisen about the thyroid peroxidase-catalyzed oxidation of the triphenylmethane class of dyes because the reactions might form various *N*-de-alkylated primary and secondary aromatic amines, with structures similar to aromatic amine carcinogens [8].

In recent years [9–14], semiconductor-assisted photocatalysis has been extensively investigated, mainly due to its capacity to degrade a high number of recalcitrant chemicals in gaseous or aqueous systems, through relatively inexpensive procedures. Photocatalysts are self-regenerated and can be used or recycled. TiO_2 is the most commonly used effective photocatalyst for a wide range of organic chemical degradation [9–13,15]. Recent studies have focused on the photocatalytic oxidation of organic pollutants mediated by TiO_2 particles in aqueous suspensions. While most photocatalytic studies have used anatase TiO_2 as photocatalyst, numerous studies [16–20] have been carried out to

* Corresponding author. Tel.: +886 4 2219 6975; fax: +886 4 2219 4990.
E-mail address: ccchen@ntcnc.edu.tw (C.C. Chen).

0021-9673/$ – see front matter © 2008 Elsevier B.V. All rights reserved.
doi:10.1016/j.chroma.2008.01.027

evaluate the potential of other metal oxides. Among others, zinc oxide appears as a very promising photocatalyst for degradation of organic solutes in aqueous systems. The quantum efficiency of ZnO powder is also significantly greater than that of TiO_2 powder. In some cases, ZnO has actually proven more effective than TiO_2 [21–23]. The ZnO-mediated photocatalysis process under UV-light irradiation has been successfully used to degrade dye pollutants for the past few years [14,24–29]. ZnO is available at low cost, which gives it an important advantage. However, the solar UV-light reaching the surface of the earth and available to excited TiO_2 is relatively small (around 4%), and artificial UV-light sources are somewhat expensive. The biggest advantage of ZnO is that it absorbs over a larger fraction of the solar spectrum than TiO_2 [30,31]. For this reason, ZnO is the most suitable photocatalyst for photocatalytic degradation when sunlight is present. Therefore, the present work focuses on exploring means to effectively utilize visible-light sources in treating dye wastewater using ZnO.

In early reports [24,25,32], most studies focused on new photocatalysts, the effects of experimental conditions, and the possibility of environmental application, not on decomposed mechanisms and intermediates under visible-light irradiation. Reports [33–37] in the literature on the photocatalytic degradation of dyes under visible light or sunlight are few. They examined the effects of various parameters like the initial concentration of substrates, amount of catalysts, and pH values. However, the mechanisms of the ZnO-assisted photocatalytic degradation of triphenylmethane dye under visible-light irradiation have never been reported.

Accordingly, this study focuses on the separation and identification of the photocatalytic reaction intermediates in hopes of shedding some light on the mechanistic details of photodegradation of MG dye in the ZnO/Vis process as a foundation for future application of this energy saving technology. Additionally, the present study also focuses on the photocatalytic degradation of simulated dyehouse effluents associated with assisting chemicals.

2. Experimental

2.1. Chemicals

MG dye (molecular formula: $C_{27}H_{35}Cl_2N_3{\cdot}xZnCl_2$, Color Index: 42590) was obtained from Acros (New Jersey, USA) and used without any further purification. The chemical structure of the MG dye is displayed in Fig. 1. The ZnO nanoparticle (particle size, ca. 50–70 nm; BET area, ca. 15–25 $m^2\ g^{-1}$) was purchased from Aldrich (USA). $Na_2S_2O_8$, H_2O_2, and Na_2CO_3 were purchased from Shimakyu (Osaka, Japan). Reagent-grade ammonium acetate, sodium hydroxide, nitric acid, and HPLC-grade methanol were purchased from Merck (Darmstadt, Germany). De-ionized water was used throughout this study.

2.2. Apparatus and instruments

The C-75 Chromato-Vue cabinet of UVP provides a wide area of illumination from the 15-W visible-light tubes positioned on two sides of the cabinet interior [38]. A Waters ZQ LC–MS system, equipped with a binary pump, a photodiode array detector (DAD), an autosampler, and a micromass detector, was used for separation and identification.

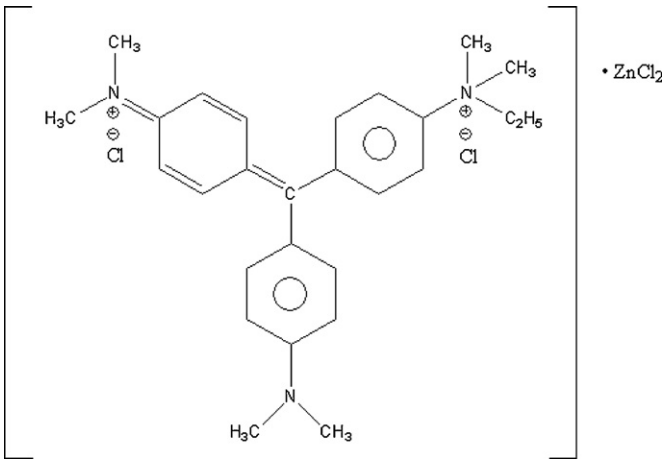

Fig. 1. Chemical structure of MG.

2.3. Experimental procedures

The irradiation experiments were carried out in a batch reactor with a 100-mL Flask (Pyrex glass) and two visible lamps (15 W). An average irradiation intensity of 4.8 W/m^2 was maintained throughout the experiments and was measured by internal radiometer. An aqueous ZnO suspension was prepared by adding 50 mg of ZnO powder to a 100 mL solution containing the MG dye at appropriate concentrations. For reactions in different pH media, the initial pH of the suspensions was adjusted by addition of either NaOH or HNO_3 solutions. Prior to irradiation, the suspensions were magnetically stirred in the dark for ca. 30 min to ensure the establishment of adsorption/desorption equilibrium. During the photocatalytic experiments, the slurry composed of dye solution and catalyst was placed in the reactor and stirred magnetically for agitation with simultaneous exposure to visible light. At specific time intervals samples were withdrawn, and to remove the ZnO particles the solution samples were centrifuged to assess the extent of decolorization and degradation by HPLC–DAD-ESI-MS.

2.4. HPLC–ESI-MS

After each irradiation cycle, the amount of the residual dye was determined by HPLC–DAD. The analysis of organic intermediates was accomplished by HPLC–ESI-MS after the readjustment of the chromatographic conditions in order to make the mobile phase compatible with the working conditions of the mass spectrometer. Two different kinds of solvents were prepared in this study. Solvent A was 25 mM aqueous ammonium acetate buffer (pH 6.9) while solvent B was methanol instead of ammonium acetate. LC was carried out on an Atlantis^{TM} dC18 column (250 mm × 4.6 mm i.d., dp = 5 μm). The flow rate of the mobile phase was set at 1.0 mL/min. A linear gradient was set as follows: $t = 0$, $A = 95$, $B = 5$; $t = 20$, $A = 50$, $B = 50$; $t = 60$, $A = 10$,

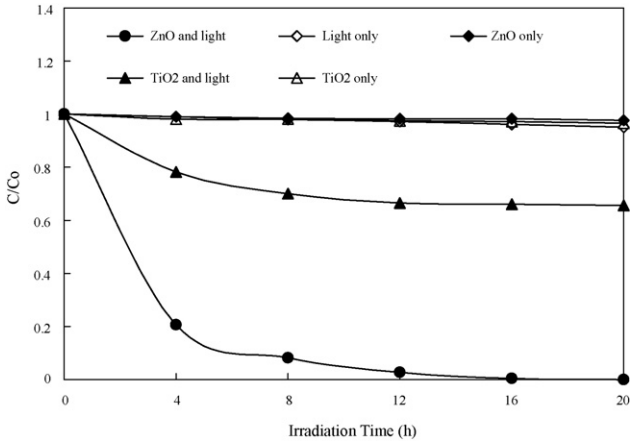

Fig. 2. Photodegradation of MG as a function of irradiation time in presence of ZnO (TiO_2) without light, light without ZnO (TiO_2), and ZnO (TiO_2) and light.

$B = 90$; $t = 65$, $A = 95$, $B = 5$. The column effluent was introduced into the ESI source of the mass spectrometer.

Equipped with an ESI interface, the quadruple mass spectrometer with heated nebulizer probe at 200 °C was used with an ion source temperature of 120 °C. ESI was carried out with the vaporizer at 200 °C and nitrogen as sheath (551 kPa) and auxiliary (138 kPa) gas to assist with the preliminary nebulization and to initiate the ionization process. A discharge current of 5 μA was applied. Cone lens and capillary voltages were optimized for the maximum response during perfusion of the MG standard.

3. Results and discussion

3.1. Control experiments

The profiles of the photocatalytic degradation of 0.05 g L^{-1} MG dye solution containing 0.5 g L^{-1} ZnO (or TiO_2) as function of irradiation time under varied conditions are illustrated in Fig. 2. A perusal of Fig. 2 shows a negligible decrease in the concentration of dye under irradiation in the absence of ZnO (or TiO_2) or in the presence of ZnO (or TiO_2) without a light source. It is evident from the figure that the photolysis of the MG solution in the presence of ZnO (or TiO_2) leads to the disappearance of the compound. The blank experiments with either illuminating MG or with the suspension containing ZnO (or TiO_2) and MG in the dark showed that both illumination and the catalyst were necessary for the destruction of dye. Therefore, we tentatively propose that MG photocatalytic degradation was performed by ZnO (or TiO_2) under visible-light irradiation. The results showed that ZnO exhibits higher photocatalytic activity than TiO_2, and the same trend was also obtained in other studies with dyes [21–23,25]. Hence, all further studies were carried out using Aldrich ZnO catalysts.

3.2. pH effect

Besides the essential role played by oxygen in generating the oxidizing species ($^{\bullet}OH$, $O_2^{\bullet -}$, H_2O_2, $HO_2^{\bullet}$), it deserves to be mentioned that transfer of the photogenerated charge carriers (and therefore, the overall degradation rate) at the semiconductor/liquid interface, is influenced to some extent by the surface properties of the semiconductor, which include pH, surface hydroxyl groups, and adsorbed charged molecules. The zero point charge for ZnO is 9.0, and above this value, the ZnO surface is predominantly negatively charged when the pH is higher than the ZnO isoelectric point. Thus, the electrical property of the ZnO surface varies with the pH of the dispersion [16].

Attempts were therefore made to study the influence of pH on the photodegradation process. Reactions were performed at different pH values using ZnO as photocatalyst. The role of pH on the photodegradation was studied in the pH range of 4–10 at a 50 mg L^{-1} dye concentration and 0.5 g L^{-1} catalyst loading. The pH of the solution was adjusted before irradiation and was not controlled during the course of the reaction. As shown in Fig. 1S of supporting information, the efficiency of the photocatalytic degradation of MG depends on the initial pH of the solution used in the reaction. The photodegradation rate was found to decrease and then increase with increases in the value of pH.

3.3. Effect of photocatalyst concentration

In slurry photocatalytic processes, the amount of photocatalyst is an important parameter. Hence, the effect of photocatalyst concentration on the photodegradation rate of the MG dye was investigated by employing different concentrations of ZnO ranging from 0.1 to 1.0 g L^{-1}. As expected, the photodegradation rate of the MG was found to increase and then decrease with the increase in the catalyst concentration (Fig. 2S of supporting information). This is a general characteristic of heterogeneous photocatalyst, and our results are in agreement with earlier reports [23]. The MG degradation rate decreases when we increase ZnO concentration above 0.25 g L^{-1}. This phenomenon may be due to the aggregation of ZnO particles at high concentrations [23], causing a decrease in the number of surface active sites. However, it is known that there exists a practical limit of the scattering light (around 1 g L^{-1}), above which the degradation rate will decrease due to the reduction of the photonic flux within the irradiated solution [33,39]. In the following experiment, we chose 0.25 g L^{-1} of ZnO as the optimum dosage under pH 10.

3.4. Effect of dye concentration

The typical textile effluent has a dye concentration ranging from 0.15 to 0.2 g L^{-1}. The effect on the degradation rate of varying the initial concentration from 0.05 to 0.25 g L^{-1} at constant catalyst loading (0.25 g L^{-1}, pH 10) could be determined, and the results are shown in Fig. 3S of supporting information. It is obvious that the degradation efficiency decreases with the increase of the initial dye concentration. This negative effect can be explained by the following reasons: as the dye concentration increases, the equilibrium adsorption of dye at the active sites on the catalyst surface increases; hence competitive adsorption of O_2 and OH^- at the same sites decreases, meaning

a lower formation rate of $O_2^{\bullet -}$ and $^{\bullet}OH$ radicals, the principal oxidants necessary for high degradation efficiency. On the other hand, according to the Beer–Lambert law, as the initial dye concentration increases, the path length of photons entering the solution decreases, resulting in lower photon adsorption on catalyst particles and, consequently, a lower photodegradation rate.

3.5. Effect of NaCl

About 70–120 g L^{-1} of NaCl is present in the typical textile effluent. The role of NaCl on the degradation rate was studied at a pH of 10, a dye concentration of 0.15 g L^{-1}, a 0.25 g L^{-1} ZnO catalyst load, and an irradiation time of 24 h. The results in Fig. 4S of supporting information show that the rate of degradation decreases with increasing NaCl concentration. The inhibition effects of anions can be explained as the reaction of hydroxyl radical with anions that behave as $^{\bullet}OH$ radical scavengers (Eq. (1)) resulting in prolonged color removal. Probably, the anions compete with MG dye for the photo-oxidizing species on the surface and prevent the photocatalytic degradation of the dyes. Formation of inorganic radical anions (e.g. $Cl_2^{\bullet -}$, $Cl^{\bullet}$) under these circumstances is possible.

$$Cl^- + {}^{\bullet}OH \rightarrow Cl^{\bullet} + OH^- \quad (1)$$

$$Cl^- + Cl^{\bullet} \rightarrow Cl_2^{\bullet -} \quad (2)$$

Although the reactivity of these radicals may be considered, they are not as reactive as $^{\bullet}OH$ due to their lower oxidation potentials [19,20,40]. Moreover, the presence of radical scavengers (Cl^-) at high doses may retard the advanced oxidation reactions drastically [28].

3.6. Effect of sodium carbonate

In fixing the dye on fabric and securing color fastness sodium carbonate is often used. Consequently, the wastewater from dyeing operations contains substantial amounts of carbonate ions. Hence, studying the effect of carbonate ions on photodegradation efficiency is important. Experiments were performed with sodium carbonate in the range of 1.0×10^{-5} to 1.0×10^{-4} M. We observed photodegradation efficiency gradually decrease with increasing amounts of carbonate ion in Fig. 5S of supporting information. This inhibition is undoubtedly due to its ability to act as a hydroxyl radical scavenger through the following reactions [41,42]:

$$^{\bullet}OH + CO_3^{2-} \rightarrow OH^- + CO_3^{\bullet -} \quad (3)$$

$$^{\bullet}OH + HCO_3^- \rightarrow H_2O + CO_3^{\bullet -} \quad (4)$$

Although, the generated carbonate radical anion has been shown to be an oxidant itself, it has less oxidation potential than the hydroxyl radicals. Hence, the presence of auxiliary chemicals like sodium carbonate in the dye solution hinders the photocatalytic degradation of dyes [40].

3.7. Effect of $Na_2S_2O_8$

NaCl and Na_2CO_3 are present in the typical textile effluent. As can be seen, increasing the concentration of Cl^- and CO_3^{2-} significantly decreases the decolorization percentage. In the following experiment, we chose 0.25 g L^{-1} of ZnO, 7 g L^{-1} NaCl, 10.6 g L^{-1} $NaCO_3$, and pH 10 as simulating textile wastewater. In early reports [43,44], an increase of $S_2O_8^{2-}$ concentration causes a surge in the reaction rate for ZnO suspensions under near neutral conditions. The effect of the electron scavenger ($S_2O_8^{2-}$) on photocatalytic degradation was investigated by varying its concentration from 1.0×10^{-5} to 1.0×10^{-4} M. The photodegradation efficiencies were found to increase and then decrease with increasing amounts of persulphate ion in Fig. 6S of supporting information. The following are the relevant reactions involving $Na_2S_2O_8$:

$$S_2O_8^{2-} + e^-_{cb} \rightarrow SO_4^{\bullet -} + SO_4^{2-} \quad (5)$$

$$SO_4^{\bullet -} + e^-_{cb} \rightarrow SO_4^{2-} \quad (6)$$

$$SO_4^{\bullet -} + H_2O \rightarrow {}^{\bullet}OH + SO_4^{2-} + H^+ \quad (7)$$

$$SO_4^{\bullet -} + Dye^+ \rightarrow\rightarrow\rightarrow SO_4^{2-} + Dye^{\bullet +} \quad (8)$$

$$Dye^{\bullet +} \rightarrow\rightarrow\rightarrow CO_2 \quad (9)$$

The excited dye injects an electron into the conduction band of ZnO, where it is scavenged by $S_2O_8^{2-}$ to form $SO_4^{\bullet -}$ as shown in Eq. (5). Obviously, the reactions in Eqs. (5) and (6) compete with electrons, which are injected from the excited dye.

The sulphate radical anion ($SO_4^{\bullet -}$) thus formed is a very strong oxidant ($E^0 = 2.6$ eV) and may react with dye [45]. It traps the photogenerated electron and/or generates hydroxyl radicals [43]. The hydroxyl radical and sulphate radical anion, being powerful oxidants, degrade the dye molecule. $SO_4^{\bullet -}$ has the unique tendency to attack dye molecule at various positions and fragment them. Further, the increase in persulphate concentration decreases the degradation rate (Fig. 6S of supporting information) by adsorpting the excess sulphate ions formed during the reaction on the surface of the ZnO and deactivating a section of the catalyst [46]. It must be noted that oxidants act not only by entrapping photogenerated electrons, but also by absorbing light and acting as sensitizers through the production of hydroxyl and sulphate radicals. Our results show that 5×10^{-5} M $Na_2S_2O_8$ is the optimal concentration to use with visible-light irradiation.

3.8. Effect of H_2O_2

The addition of an oxidant into a semiconductor suspension has been proven to enhance the degradation rate of the organic pollutant [46–48]. The photocatalytic degradation of MG found to be severely affected by the addition of hydrogen peroxide. On adding H_2O_2 in the concentration range of 1.0×10^{-5} to 1.0×10^{-3} M, values for degradation efficiency first increase quickly then decrease as shown in Fig. 7S of supporting information. The initial increase in reaction efficiency that accompanies the addition of H_2O_2 can be attributed to the formation of $^{\bullet}OH$ radicals responsible for the photocatalytic oxidation.

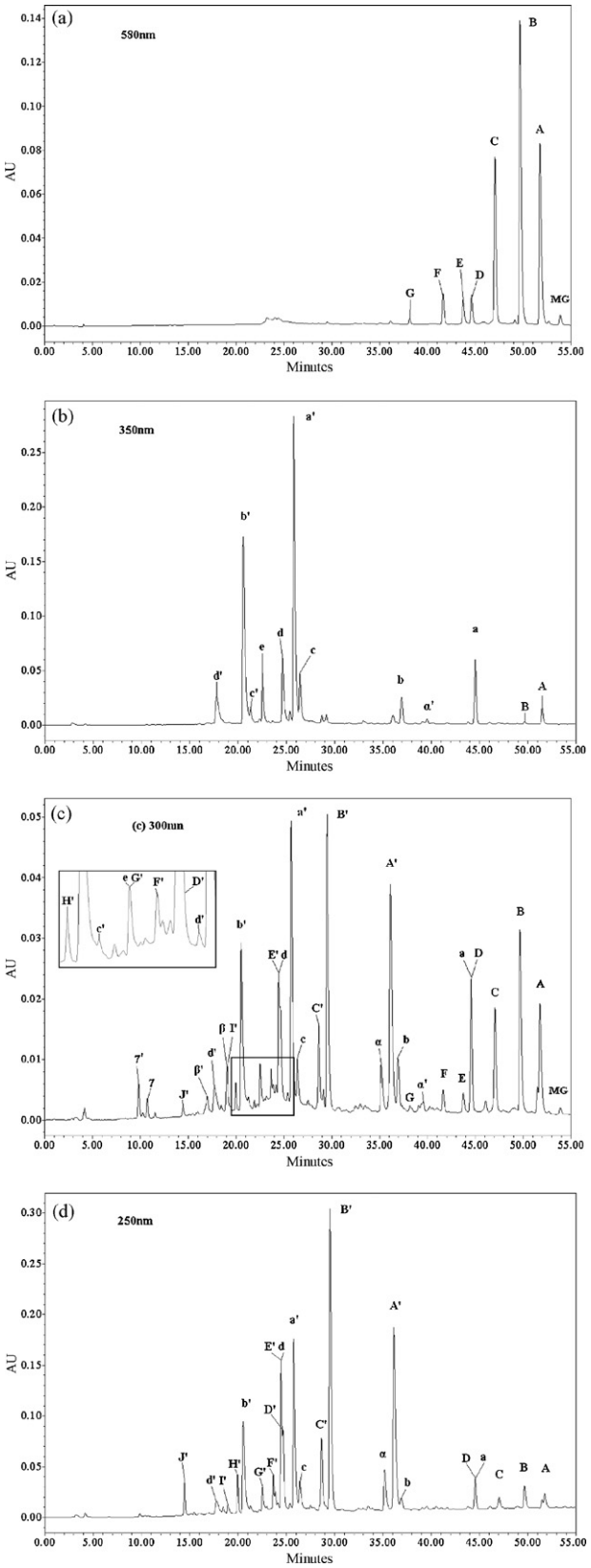

Fig. 3. HPLC chromatogram of the intermediates with ZnO 0.25 g L^{-1}, at pH 10, at 12 h of irradiation, recorded at (a) 580 nm, (b) 350 nm, (c) 300 nm, and (d) 250 nm.

Table 1
The nomenclature of the intermediates of the photodegradation MG

Compounds	Intermediates
MG	*N*-Ethyl-*N,N,N′,N′,N″,N″*-hexamethylpararosaniline
A	*N,N*-Dimethyl-*N′,N′*-dimethyl-*N″,N″*-dimethylpararosaniline
B	*N,N*-Dimethyl-*N′,N′*-dimethyl-*N″*-methylpararosaniline
C	*N,N*-Dimethyl-*N′*-methyl-*N″*-methylpararosaniline
D	*N,N*-Dimethyl-*N′,N′*-dimethylpararosaniline
E	*N*-Methyl-*N′*-methyl-*N″*-methylpararosaniline
F	*N,N*-Dimethyl-*N′*-methylpararosaniline
G	*N*-Methyl-*N′*-methylpararosaniline
H	*N,N*-Dimethylpararosaniline
I	*N*-Methylpararosaniline
J	Pararosaniline
A′	[4-(*N*-Ethyl-*N,N*-dimethylamino)][4′-(*N′,N′*-dimethylamino)][4″-(*N″,N″*-dimethylamino)]triphenylmethanol
B′	[4-(*N*-Ethyl-*N,N*-dimethylamino)][4′-(*N′,N′*-dimethylamino)][4″-(*N″*-methylamino)]triphenylmethanol
C′	[4-(*N*-Ethyl-*N*-methylamino)][4′-(*N′,N′*-dimethylamino)][4″-(*N″,N″*-dimethylamino)]triphenylmethanol
D′	[4-(*N*-Ethyl-*N,N*-dimethylamino)][4′-(*N′*-methylamino)][4″-(*N″*-methylamino)]triphenylmethanol
E′	[4-(*N*-Ethyl-*N,N*-dimethylamino)][4′-(*N′,N′*-dimethylamino)][4″-(amino)]triphenylmethanol
F′	[4-(*N*-Ethyl-*N*-methylamino)][4′-(*N′,N′*-dimethylamino)][4″-(*N″*-methylamino)]triphenylmethanol
G′	[4-(*N*-Ethylamino)][4′-(*N′,N′*-dimethylamino)][4″-(*N″,N″*-dimethylamino)]triphenylmethanol
H′	[4-(*N,N*-Dimethylamino)][4′-(*N′,N′*-dimethylamino)][4″-(*N″,N″*-dimethylamino)]triphenylmethanol
I′	[4-(*N*-Ethyl-*N*-methylamino)][4′-(*N′*-methylamino)][4″-(*N″*-methylamino)]triphenylmethanol
J′	[4-(*N*-Ethyl-*N,N*-dimethylamino)][4′-(*N′*-methylamino)][4″-(amino)]triphenylmethanol
a	4-(*N,N*-Dimethylamino)-4′-(*N′,N′*-dimethylamino)benzophenone
b	4-(*N,N*-Dimethylamino)-4′-(*N′*-methylamino)benzophenone
c	4-(*N*-Methylamino)-4′-(*N′*-methylamino)benzophenone
d	4-(*N,N*-Dimethylamino)-4′-aminobenzophenone
e	4-(*N*-Methylamino)-4′-aminobenzophenone
a′	4-(*N*-Ethyl-*N,N*-dimethylamino)-4′-(*N′,N′*-dimethylamino)benzophenone
b′	4-(*N*-Ethyl-*N,N*-dimethylamino)-4′-(*N′*-methylamino)benzophenone
c′	4-(*N*-Ethyl-*N*-methylamino)-4′-(*N′,N′*-dimethylamino)benzophenone
d′	4-(*N*-Ethyl-*N*-methylamino)-4′-(*N′*-methylamino)benzophenone
α	4-(*N,N*-Dimethylamino)phenol
β	4-(*N*-Methylamino)phenol
γ	4-Aminophenol
α′	4-(*N*-Ethyl-*N,N*-dimethylamino)phenol
β′	4-(*N*-Ethyl-*N*-methylamino)phenol
γ′	4-(*N*-Ethylamino)phenol

Table 2
Identified photodegradation products and their main fragments determined by LC–DAD-ESI-MS

Peaks	Compounds	Retention time (min)	$[M+H^+]$	ESI-MS spectrum (*m/z*) ions	Absorption maximum (nm)
MG	EDDD-PR; MG	54.89	200.08		588.3
A	DDD-PR	51.88	372.56		589.3
B	DDM-PR	49.82	358.49		582.0
C	DMM-PR	47.24	344.37		574.6
D	DD-PR	45.13	344.50		579.5
E	MMM-PR	44.07	330.37		563.6
F	DM-PR	42.04	330.43		570.9
G	MM-PR	38.73	316.37	238.48	563.6
a	DDBP	45.15	269.39	241.40	374.0
b	DMBP	34.52	255.39	223.38, 210.29	372.8
c	MMBP	24.87	241.33	212.17	363.1
d	DBP	24.68	241.46	195.90	366.7
e	EBP	21.73	227.46	197.26	360.1
A′	EDDD-TPM	36.61	418.50	372.43, 269.46	259.5
B′	ED-DM-TPM	29.96	404.50	358.49, 255.46	254.8
C′	EM-DD-TPM	29.16	404.57	358.49, 255.33	254.8
D′	ED-MM-TPM	25.09	390.44	344.50, 269.46, 241.27	249.4
E′	ED-D-TPM	24.79	390.51	344.50, 255.46	251.3
F′	EM-DM-TPM	24.02	390.57	258.43, 255.52	250.5
G′	E-DD-TPM	23.89	390.44	258.43, 314.49, 255.52	251.1
H′	D-DD-TPM	19.779	390.27	344.37, 255.26	249.9
I′	EM-MM-TPM	19.45	376.44	344.56, 255.52	245.8
J′	ED-M-TPM	19.78	376.51	344.43	247.1
a′	ED-DBP	26.71	297.52	268.42, 224.22	374.0
b′	ED-MBP	20.71	283.52	245.36, 210.29	362.1
c′	EM-DBP	20.96	283.39	254.42, 210.29	360.1
d′	ED-BP	17.86	269.20	253.12, 224.48	360.4
α	DAP	39.20	138.09	126.70	296.4
β	MAP	19.45	124.10	109.26	289.2
γ	AP	10.74	N/A		280.9
α′	EDAP	37.01	166.72		297.2
β′	EMAP	17.02	N/A		291.8
γ′	EAP	9.89	N/A		289.4

Hydroxyl radicals have 2.05 and 1.58 times more oxidizing power than chlorine and H_2O_2, respectively. H_2O_2 increases the rate of hydroxyl radical formation in three ways: first, the Eq. (10) depicts the reduction of H_2O_2 at the conductance band would also produce hydroxyl radicals. Secondly, even if H_2O_2 was not reduced at the conductance band, it could accept an electron from the superoxide, again producing hydroxyl radicals (Eq. (11)).

$$e^-_{cb} + H_2O_2 \rightarrow OH^- + {}^\bullet OH \quad (10)$$

$$O_2{}^{\bullet -} + H_2O_2 \rightarrow OH^- + {}^\bullet OH + O_2 \quad (11)$$

At high concentrations, the hydrogen peroxide adsorbed on the photocatalytic surface could effectively scavenge the $^\bullet$OH radicals formed on the photocatalytic surface. (Eqs. (12) and (13)) and thus inhibit the major pathway for heterogeneous generation of $^\bullet$OH radicals [49]:

$$^\bullet OH + H_2O_2 \rightarrow H_2O + HO_2{}^\bullet \quad (12)$$

$$HO_2{}^\bullet + {}^\bullet OH \rightarrow H_2O + O_2 \quad (13)$$

It is worth mentioning here that $HO_2{}^\bullet$ radicals are less reactive than $^\bullet$OH, and, therefore, make a negligible contribution to the dye degradation. From the results reported above it is clear that 1×10^{-4} M H_2O_2 is the optimal concentration.

3.9. Evolution of UV–Vis spectra

The changes of the UV–Vis spectra during the photodegradation process of the MG dye are illustrated in Fig. 8S of supporting information. Under visible-light irradiation, the MG dye can be degraded efficiently in aqueous MG/ZnO dispersions. About 99.9% of the MG dye was degraded after irradiation for 16 h. The characteristic absorption band of the dye around 588.1 nm decreased rapidly with a slight hypsochromic shift (584.3 nm) (Fig. 8S of supporting information). Similar results were also observed during the TiO_2/Vis photocatalytic degradation of ethyl violet [50], and crystal violet [51].

3.10. Separation of the intermediates

Using a low intensity lamp enabled us to obtain slower degradation rates and provide favorable conditions for the determination of intermediates using HPLC–DAD-ESI-MS. The dye and its related intermediates are marked as species **A–G**, **a–e**, **a′–d′**, **α–γ**, **α′–γ′**, and **A′–J′** in the chromatograms (Fig. 3),

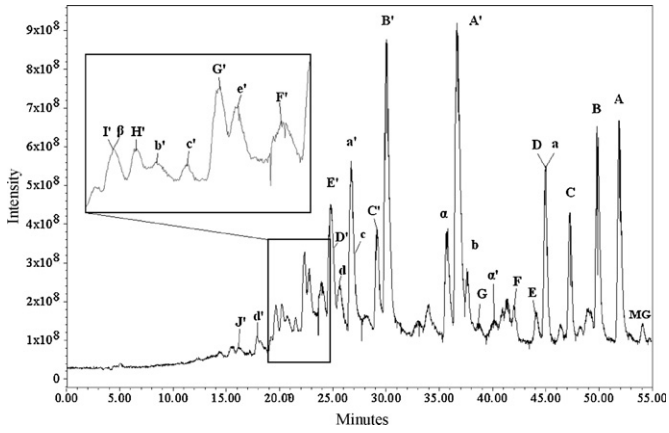

Fig. 4. Total ion chromatogram of the photodegraded intermediates with 12 h of irradiation.

recorded at 580, 350, 300, and 250 nm. Thirty-two components were identified, with irradiation up to 12 h at pH 10 and retention time of less than 55 min. Except for the initial MG dye, the intensity of other peaks increased at first and subsequently decreasing, indicating formation and transformation of the intermediates.

3.11. Identification of the intermediates

3.11.1. Absorption spectra of the intermediates

Absorption spectra of photodegraded intermediates of MG dye, corresponding to the peaks observed in Fig. 3, are shown in Fig. 9S of supporting information. From these spectra, several categories of intermediates can be distinguished as follows.

The nomenclature of the intermediates we observed above can be seen more clearly in Table 1. The first category of intermediates have the wavelength position of its major absorption band moved toward the blue region, λ_{max}, **A**, 589.3 nm; **B**, 582.0 nm; **C**, 574.6 nm; **D**, 579.5 nm; **E**, 563.6 nm; **F**, 570.9 nm; **G**, 563.6 nm. These intermediates may be the *N*-de-methylation of the crystal violet (CV) dye. Similar phenomena were also observed during the TiO_2-mediated photodegradation of CV [51]. The second categories of intermediates produced by cleavage of the CV chromophore ring structure, *N*-de-methylation of the DDBP (**a**), have the wavelength position of its major absorption band moved toward the blue region, λ_{max}, **a**, 374.0 nm; **b**, 372.8 nm; **c**, 363.1 nm; **d**, 366.7 nm; **e**, 360.1 nm. These intermediates were also observed during the TiO_2-mediated photodegradation of Michler's ethyl ketone [52]. The third categories of intermediates produced by cleavage of the CV chromophore ring structure, *N*-de-methylation of the DAP (**α**), have the wavelength position of its major absorption band moved toward the blue region, λ_{max}, **α**, 296.4 nm; **β**, 289.2 nm; **γ**, 280.9 nm. Similar phenomena were also observed during the ZnO-mediated photodegradation of ethyl violet [23].

The fourth categories of intermediates produced by cleavage of the carbinol base (CB; triarylmethanol), *N*-de-alkylation of the EDDBP (**a′**), have the wavelength position of its major absorption band moved toward the blue region, λ_{max}, **a′**, 374.0 nm; **b′**, 362.1 nm; **c′**, 360.1 nm; **d′**, 360.4 nm. The fifth

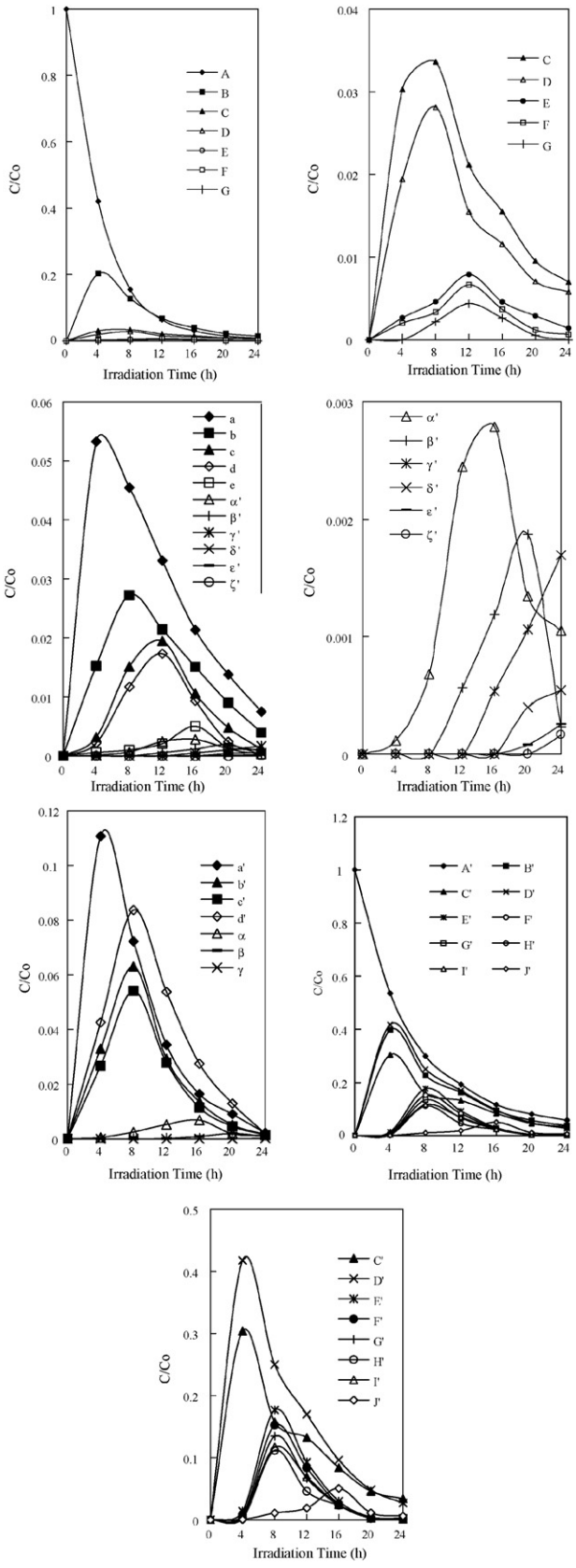

Fig. 5. Variation in the relative distribution of the intermediates obtained from the photodegradation of the MG dye as a function of the irradiation time. Curves A–G, A′–J′, a–e, a′–d′, α–β, and α′ corresponds to the peaks **A–G**, **A′–J′**, **a–e**, **a′–d′**, **α–β**, and **α′** in Fig. 3, respectively.

categories of intermediates produced by cleavage of the CB, *N*-de-alkylation of the EDAP (**α′**), have the wavelength position of its major absorption band moved toward the blue region, λ_{max}, **α′**, 297.2 nm; **β′**, 291.8 nm; **γ′**, 289.4 nm. The sixth categories of intermediates produced by *N*-de-alkylation of the CB have the wavelength position of its major absorption band moved toward the blue region, λ_{max}, **A′**, 259.5 nm; **B′**, 254.8 nm; **C′**, 254.8 nm; **D′**, 249.4 nm; **E′**, 251.3 nm; **F′**, 250.5 nm; **G′**, 251.1 nm; **H′**, 249.9 nm; **I′**, 245.8 nm; **J′**, 247.1 nm. These intermediates were also observed during the TiO_2-mediated photodegradation of methyl green [53]. The nomenclature of the intermediates and data we observed above can be seen more clearly in Tables 1 and 2.

3.11.2. Mass spectra of the intermediates

The intermediates are further identified using the HPLC–ESI-MS. ESI mass spectra are shown in Fig. 10S of supporting information and the total ion chromatogram is illustrated in Fig. 4. The molecular ion peaks appeared to be the acid forms of the intermediates. Results of HPLC–ESI mass spectra are summarized in Table 2.

3.12. Evolution of intermediates

The evolutions of the initial dye concentration and of the identified intermediates were followed as a function of irradiation time. The result is displayed in Fig. 5. The *N*-mono-de-methylated intermediate (**B**) was clearly observed (Fig. 5, curve B) to reach its maximum concentration after a 4 h irradiation period. The other *N*-methylated intermediates, **C**, **D**, **E**, **F**, and **G** were clearly observed (curves C–G) to reach their maximum concentrations after 8-, 8-, 12-, 12-, and 12-h irradiation periods, respectively.

The oxidative degradation intermediates, **a** and **α**, were clearly observed (Fig. 5, curves a and α) to reach their maximum concentrations after a 4- and 16-h irradiation period. The *N*-mono-de-methylated intermediates **b** and **β** were clearly observed (curves b and β) to reach their maximum concentrations after an 8- and 20-h irradiation period. The other *N*-de-methylated intermediates **c–e** and **γ** were clearly observed (curves c–e and γ) to reach their maximum concentrations after a 12-, 12-, 16-, and 20-h irradiation period, respectively. CV is adsorbed on the TiO_2 particle surface via a conjugated structure, with the major photo-oxidation products being **a**, **α**, and their *N*-de-methylated products.

The *N*-de-alkylation of the CB occurs mostly through attack by the •OH species on the *N*,*N*-dimethyl group or *N*,*N*-dimethyl-*N*-ethyl group of CB. The *N*-mono-de-alkylated intermediates (**B′**, **C′**, **D′**) were clearly observed (Fig. 5, curves B′, C′, D′) to reach its maximum concentration at the same time after a 4-h irradiation period. The other *N*-ethylated intermediates, **E′**–**J′**, were clearly observed (curves E′–J′) to reach their maximum concentrations after 8-, 8-, 8-, 8-, 8-, and 16-h irradiation periods, respectively.

The oxidative degradation of the CB dye occurs mostly through attack by the •OH species on the central carbon portion of CB and produces two sets of intermediates, **a** and **α**, and **a′** and **α′**, under basic aqueous conditions. The oxidative degradation of two sets of intermediates was clearly observed (Fig. 5, curves a, α, a′, and α′) to reach their maximum concentrations after a 4-, 16-, 4-, and 16-h irradiation period, respectively. The other oxidative intermediates (**b–e**, **β–γ**, **b′–d′**, and **β′–γ′**) were clearly observed (curves b–e, β–γ, b′–d′, and β′–γ′) to reach their maximum concentrations after 8-, 12-, 12-, 16-, 20-, 20-, 8-, 8-, 8-, 20-, and 24-h irradiation periods, respectively.

The concentration of the other intermediates may be under the detectable limit. To minimize errors, the relative intensities were recorded at the maximum absorption wavelength for each intermediate, although a quantitative determination of all of the photogenerated intermediates was not achieved, owing to the lack of appropriate molar extinction coefficients for them and to unavailable reference standards.

3.13. Degradation mechanisms of MG

According to all the above experimental results, we tentatively propose the pathway of degradation depicted in Fig. 6. Under pH 10, the cationic MG dye molecules are converted into the colorless CB, which is tertiary alcohol, and CV dye by hydroxide anion. Then, CV and CB are degraded by the photocatalyst, ZnO. These phenomena have been reported in our recent reports [53] relating to TiO_2-mediated photocatalytic degradation under UV irradiation.

Under visible-light irradiation, most of the •OH radicals are generated directly from the reaction between the $O_2^{\bullet -}$ subsequently reacts with H_2O [32]. CV gets near the negatively charged TiO_2 particle surface via the positive dimethylamine group. The *N*-de-methylation of the CV dye occurs mostly through attack by the •OH species on the *N*,*N*-dimethyl portion of CV. The successive appearance of the maximum of each intermediate indicates that the *N*-de-methylation (Eq. (14)) of CV is a stepwise photochemical process.

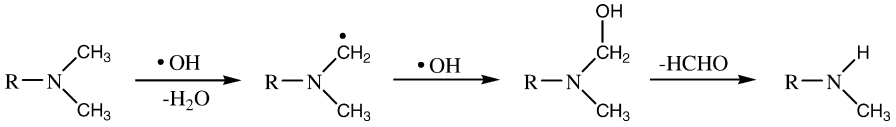

(14)

The detailed degradation pathway is presented in Fig. 6.

CV is adsorbed on the TiO_2 particle surface via a conjugated structure, with the major photo-oxidation products being DDBP, DAP, and their *N*-de-methylated products. The oxidative degradation of the CV dye occurs mostly through attack by the •OH species on the central carbon portion of CV and produces DDBP and DAP (Eq. (15)). The results we discussed above can be seen

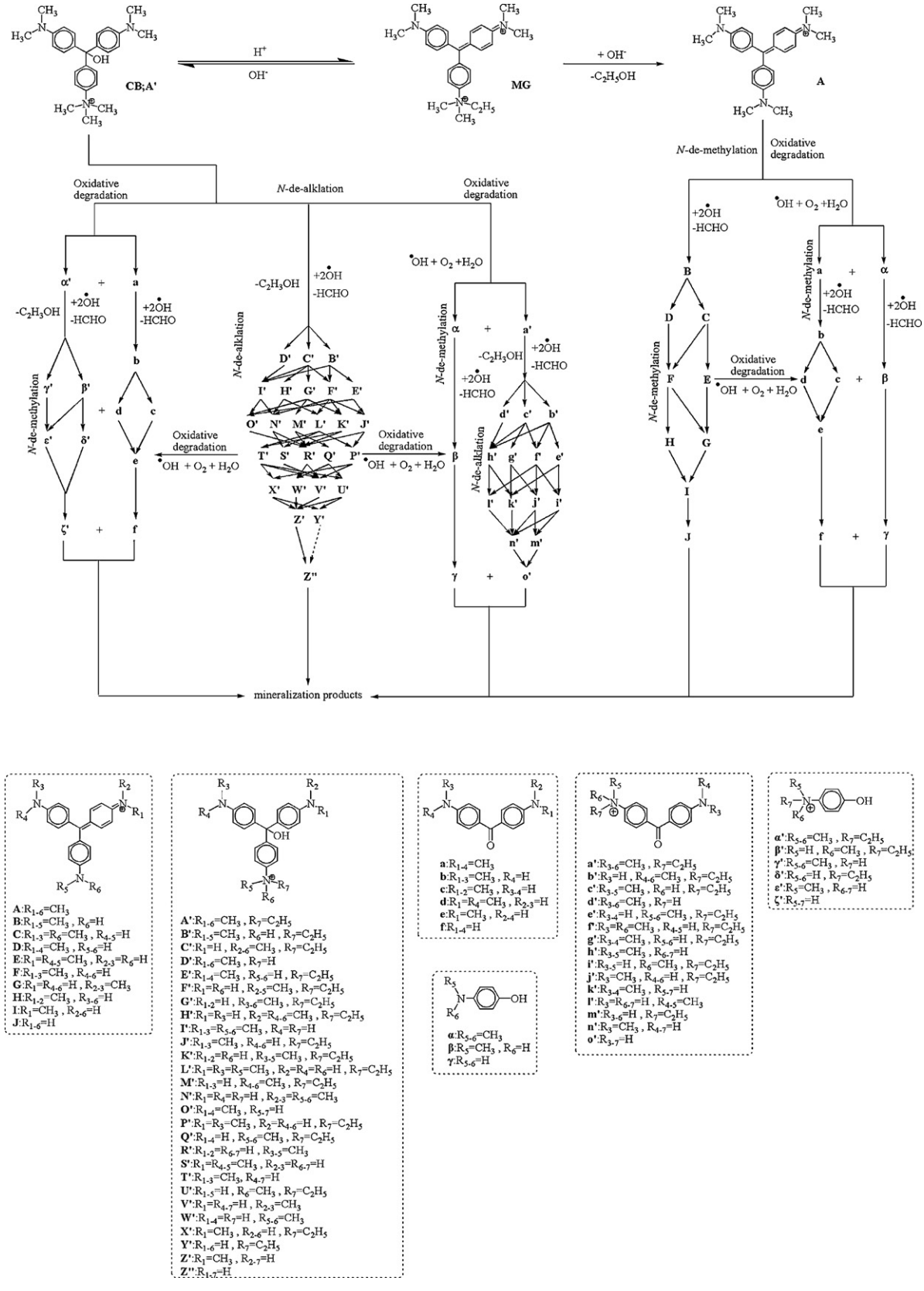

Fig. 6. Proposed pathway of MG in suspension of ZnO irradiated by visible-light under basic solution (pH 10).

more clearly from Fig. 6.

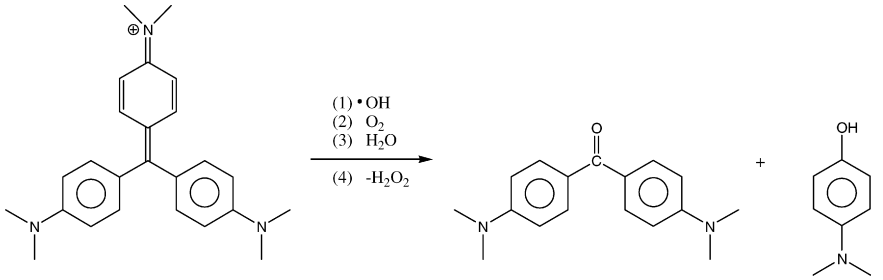

(15)

The *N*-de-alkylation of the CB occurs mostly through attack by the •OH species on the *N*,*N*-dimethyl group or *N*,*N*-dimethyl-*N*-ethyl group of CB. The relative distribution of all of the intermediates obtained is illustrated in Fig. 5. The successive appearance of the maximal quantity of each intermediate indicates that the *N*-de-ethylation of CB is a stepwise photochemical process. The results discussed above can be seen more clearly from Fig. 6.

The oxidative degradation of the CB dye occurs mostly through attack by the •OH species on the central carbon portion of CB and produces two sets of intermediates, DDBP and EDAP, and ED-DBP and DAP, under basic aqueous conditions. The evolutions of the initial dye concentration and of the identified intermediates were followed as a function of irradiation time. The result is displayed in Fig. 5. The results we discussed above can be seen more clearly from Fig. 6.

All the intermediates identified in the study were also identified in a previous study of the MG/TiO_2/UV-system [53]. Under UV irradiation, the initial step in semiconductor-mediated photocatalyzed degradation with light energy greater than the band gap energy of the semiconductor is proposed to involve the generation of a (e^-/h^+) pair leading to the formation of hydroxyl radical (•OH), superoxide radical anions ($O_2^{\bullet -}$). These radicals are the oxidizing species in the photocatalytic oxidation processes [24].

$$\mathrm{Dye}^{\bullet +} + {}^{\bullet}\mathrm{OH} \rightarrow \text{hydroxyl intermediates} \rightarrow \text{degraded products} \quad (16)$$

Under visible irradiation, early reports [45,46] depict the absorption of light by the dye molecules. The excited dye injects an electron into the conduction band of ZnO, where it is scavenged by O_2 to form $O_2^{\bullet -}$. De-alkylation of MG dye occurs mostly through attack by the species, which is a perfect nucleophilic reagent, on the *N*-alkyl portion of MG. Further $O_2^{\bullet -}$ subsequently react with H_2O to generate •OH radical and the other active radical. The probability for the formation of •OH should be much lower than for that $O_2^{\bullet -}$. The •OH is an extremely strong, non-selective oxidant, which leads to the partial or complete mineralization of several organic chemicals. All the above active radicals drive the photodegradation or mineralization of the dye molecule.

According to earlier reports [54–59], the *N*-de-alkylation processes are preceded by the formation of a nitrogen-centered radical while destruction of dye chromophore structures is preceded by the generation of a carbon-centered radical. Consistent with this, degradation of CV and CB must occur via two different photo-oxidation pathways (destruction of the structure and *N*-de-alkylation) due to the formation of different radicals (either a carbon-centered or nitrogen-centered radical) at pH 10. There is no doubt that the •OH attack on the dye yields a dye cationic radical. After this step, the cationic radical $\mathrm{Dye}^{\bullet +}$ can undergo hydrolysis and/or use various deprotonation pathways, which in turn are determined by the different adsorption modes of CV and CB on the ZnO particle surface. In weak acidic and neutral solutions, the degradation of dye has been examined. Both *N*-de-alkylation and degradation of the MG dye take place in presence of ZnO particles. These phenomena have been reported in some recent reports [54,56] relating to TiO_2-mediated photocatalytic degradation. We will not discuss those similar results here.

4. Conclusion

At low watt irradiation, MG could be successfully decolorized and degraded by ZnO under visible-light irradiation. We chose 0.25 g L^{-1} of ZnO as the optimum dosage under pH 10. NaCl and Na_2CO_3 are present in the typical textile effluent. As can be seen, increasing the concentration of Cl^- and CO_3^{2-} significantly decreases the decolorization percentage. The addition of an oxidant ($Na_2S_2O_8$ or H_2O_2) into a ZnO suspension has been proven to enhance the degradation rate of the MG pollutant. Our results show that 5×10^{-5} M $Na_2S_2O_8$ (or 1×10^{-4} M H_2O_2) is the optimal concentration to use with visible-light irradiation. Under basic aqueous conditions, the cationic MG dye molecules are converted into the colorless CB and CV dye and ethanol. Consistent with this, degradation of CV and CB must occur via two different pathways (oxidative degradation and *N*-de-alkylation) to form different intermediates by a optimal separation and identification condition of HPLC–DAD-ESI-MS.

Acknowledgments

The project was financially supported by NSC 95-2113-M-438-001 of the National Science Council of the Republic of China. The authors thank the National Taichung Nursing College for other support.

Appendix A. Supplementary data

Supplementary data associated with this article can be found, in the online version, at doi:10.1016/j.chroma.2008.01.027.

References

[1] Ullmann's Encyclopedia of Industrial Chemistry. Part A27. Triarylmethane and Diarylmethane Dyes, 6th ed., Wiley–VCH, New York, 2001.
[2] D.F. Duxbury, Chem. Rev. 93 (1993) 381.
[3] T. Inoue, K. Kikuchi, K. Hirose, M. Iiono, T. Nagano, Chem. Biol. 8 (2001) 9.
[4] F.J. Green, The Sigma–Aldrih Handbook of Stains, Dyes, and Indicators, Aldrich Chemical, Milwaukee, WI, 1990, 766 pp.
[5] T. Geethakrishnan, P.K. Palanisamy, Optik 117 (2006) 282.
[6] J. Melnick, M. Pickering, Biochem. Int. 16 (1988) 69.
[7] R. Bonnett, G. Martinez, Tetrahedron 57 (2001) 9513.
[8] B.P. Cho, T. Yang, L.R. Blankenship, J.D. Moody, M. Churchwell, F.A. Bebland, S.J. Culp, Chem. Res. Toxicol. 16 (2003) 285.
[9] A.L. Linsebigler, G.Q. Lu, J.T. Yates, Chem. Rev. 95 (1995) 735.
[10] M.A. Fox, M.T. Dulay, Chem. Rev. 93 (1993) 341.
[11] A. Hagfeldt, M. Gratzel, Chem. Rev. 95 (1995) 49.
[12] M.R. Hoffman, S.T. Martin, W. Choi, W. Bahnemann, Chem. Rev. 95 (1995) 69.
[13] T.T. Thompson, J.T. Yates, Chem. Rev. 106 (2006) 4428.
[14] K.K. Ioannis, A.A. Triantafyllos, Appl. Catal. B: Environ. 49 (2004) 1.
[15] D. Chatterjee, S. Dasgupta, J. Photochem. Photobiol. C: Photochem. Rev. 6 (2005) 186.
[16] N. Daneshvar, D. Salari, A.R. Khataee, J. Photochem. Photobiol. A 162 (2004) 317.
[17] S. Abbruzzetti, M. Carcelli, P. Pelagatti, D. Rominga, C. Viappiani, Chem. Phys. Lett. 344 (2001) 387.
[18] J. Fernandez, M. Kiwi, C. Lizama, J. Freer, J. Baeza, H.D. Mansilla, J. Photochem. Photobiol. A 151 (2002) 213.
[19] V. Nadtochenko, J. Kiwi, Inorg. Chem. 37 (1998) 5233.
[20] I. Arslan, I. Akmehmet, D.W. Bahnemann, Appl. Catal. B 26 (2000) 193.
[21] H. Lachheb, E. Puazenat, A. Houas, M. Ksibi, E. Elaloui, C. Guillard, J.M. Herrman, Appl. Catal. B: Environ. 39 (2002) 75.
[22] V. Kandavelu, H. Kastien, K.R. Thampi, Appl. Catal. B: Environ. 48 (2004) 101.
[23] C.C. Chen, J. Mol. Catal. A: Chem. 264 (2006) 82.
[24] A. Akyol, H.C. Yatmaz, M. Bayramoblu, Appl. Catal. B: Environ. 54 (2004) 19.
[25] C.G. Silva, J.L. Faria, J. Photochem. Photobiol. A: Chem. 155 (2003) 133.
[26] D. Yu, R. Cai, Z. Liu, Spectrochem. Acta A 60 (2004) 1617.
[27] A. Akyol, M. Bayramoglu, J. Hazard. Mater. B 124 (2005) 241.
[28] M.J. Height, S.E. Pratsinis, O. Mekasuwandumrong, P. Praserthdam, Appl. Catal. B: Environ. 63 (2006) 305.
[29] K. Mehrotra, G.S. Yablonsky, A.K. Ray, Ind. Eng. Chem. Res. 42 (2003) 2273.
[30] S. Sakthivel, B. Neppolian, M. Palanichamy, B. Arabindoo, V. Murugesan, Indian J. Chem. Technol. 6 (1999) 161.
[31] I. Poulios, I. Tsachpinis, J. Chem. Technol. Biotechnol. 74 (1999) 349.
[32] P.V. Kamat, B. Patrick, J. Phys. Chem. 96 (1992) 6829.
[33] S. Chakrabarti, B.K. Dutta, J. Hazard. Mater. B 112 (2004) 269.
[34] M.L. Curri, R. Comparelli, P.D. Cozzoli, G. Mascolo, A. Agostiano, Mater. Sci. Eng. C 23 (2003) 285.
[35] R. Suarez-Parra, I. Hernandez-Perez, M.E. Rincon, S. Lopez-Ayala, M.C. Roldan-Ahumada, Solar Enegry Mater. Solar Cells 76 (2003) 189.
[36] A. Pandurangan, P. Kamala, S. Uma, M. Palanichamy, V. Murugesan, Indian J. Chem. Technol. 8 (2001) 496.
[37] P.V. Kamat, R. Huehn, R. Nicolaescu, J. Phys. Chem. 106 (2002) 788.
[38] C.C. Chen, C.S. Lu, F.D. Mai, C.S. Weng, J. Hazard. Mater. B 137 (2006) 1600.
[39] N. Sobana, M. Swaminathan, Sep. Purif. Technol. 56 (2007) 101.
[40] J. Kiwi, A. Lopez, V. Nadtochenko, Environ. Sci. Technol. 34 (2000) 2162.
[41] M.A. Behnajady, N. Modirshahla, R. Hamzavi, J. Hazard. Mater. B 133 (2006) 226.
[42] M. Bekbolet, I. Balcioglu, Water Sci. Technol. 34 (1996) 73.
[43] E. Evgenidou, K. Fytianos, I. Poulios, Appl. Catal. B 59 (2005) 81.
[44] A.R. Fernandez-Alba, D. Hernado, A. Aguera, J. Caceres, S. Malato, Water Res. 36 (2002) 4255.
[45] Z. Sun, Y. Chen, Q. Ke, Y. Yang, J. Yuan, J. Photochem. Photobiol. A: Chem. 149 (2002) 169.
[46] N. Daneshvar, D. Salari, A.R. Khataee, J. Photochem. Photobiol. A: Chem. 162 (2004) 317.
[47] M. Munner, D. bahnemann, Appl. Catal. B: Enviorn. 36 (2002) 95.
[48] T. Velegraki, I. Poulios, M. Charalabaki, N. kalogerakis, P. Samaras, D. Mantzavinos, Appl. Catal. B 62 (2006) 159.
[49] I. Poulios, I. Awtopoulou, J. Environ. Technol. 20 (1999) 479.
[50] C.C. Chen, C.S. Lu, Y.C. Chung, J. Photochem. Photobiol. A: Chem. 181 (2006) 120.
[51] C.C. Chen, H.J. Fan, C.S. Lu, C.Y. Jang, J.L. Jan, H.D. Lin, J. Photochem. Photobiol. A: Chem. 184 (2006) 147.
[52] C.S. Lu, C.C. Chen, F.D. Mai, Y.C. Wu, J. Photochem. Photobiol. A: Chem. (187) (2007) 167.
[53] C.C. Chen, C.S. Lu, Environ. Sci. Technol. 41 (2007) 4389.
[54] G. Liu, T. Wu, J. Zhao, H. Hidaka, N. Serpone, Environ. Sci. Technol. 33 (1999) 2081.
[55] F.C. Shaefer, W.D. Zimmermann, J. Org. Chem. 35 (1970) 2165.
[56] J. Zhao, T. Wu, K. Wu, K. Oikawa, H. Hidaka, N. Serpone, Environ. Sci. Technol. 32 (1998) 2394.
[57] G. Galliani, B. Rindone, C. Scolastico, Tetrahedron Lett. 16 (1975) 1285.
[58] G.N. Lewis, D. Lipkin, T.T. Nagel, J. Am. Chem. Soc. 66 (1944) 1579.
[59] L.E. Manring, K.S. Peters, J. Phys. Chem. 88 (1984) 3516.